
Bridging the Generalization Gap: Training Robust Models on Confounded Biological Data

Tzu-Yu Liu*, Ajay Kannan*, Adam Drake, Marvin Bertin, Nathan Wan
Freenome Inc.

South San Francisco, CA

{joyce.liu, ajay.kannan, adam.drake, marvin.bertin, nwan}@freenome.com

Abstract

Statistical learning on biological data can be challenging due to confounding variables in sample collection and processing. Confounders can cause models to generalize poorly and result in inaccurate prediction performance metrics if models are not validated thoroughly. In this paper, we propose methods to control for confounding factors and further improve prediction performance. We introduce OrthoNormal basis construction In cOnfounding factor Normalization (ONION) to remove confounding covariates and use the Domain-Adversarial Neural Network (DANN) to penalize models for encoding confounder information. We apply the proposed methods to simulated and empirical patient data and show significant improvements in generalization.

1 Introduction

Confounding is most likely to occur when incomplete understanding of the data generation process renders factoring out confounding signal difficult. Biological datasets derived from patient samples are prone to confounding due to artifactual differences in sample collection [1]. Consider a binary classification problem, where positive and negative samples are sourced from hospital A and B, respectively. It becomes unclear if a classifier is predicting class labels or the source hospital. Stratified sampling to control for confounding variables is often infeasible due to sample procurement difficulties, lab processing batch effects, and incomplete knowledge of potential confounders. As Leek et al. pointed out, these often overlooked batch effects could result in incorrect conclusions [2]. A recent study also highlighted that performance metrics in cancer detection using sequencing data can be inaccurate when using standard k-fold cross-validation due to sequencing batch effects and sample sourcing biases [3]. Confounding is a known problem [4, 5], but it is often difficult to detect or correct, and requires careful consideration when applying machine learning methods [6].

Since stratifying samples by confounders is often infeasible, correcting the resulting biases in model inputs and representations is an important area of open research. There has been previous work on bias correction in sequencing data, including Hidden Covariates with Prior [7] and ComBat [8], which use covariate labels to normalize sequencing data. However, these methods require test set covariate labels and model re-fitting at test time, which make freezing and presenting a model for regulatory review and validation on previously unseen populations challenging. There are also domain knowledge-based sequencing technical bias correction methods, such as LOWESS GC bias correction [9, 10]. Our methods perform equivalently without relying on domain knowledge, and can be applied to generic machine learning problems.

To avoid models learning confounders, we build transformations such that samples are less confounded in the transformed space. Our goal is to find a function f such that the image $f(X)$ enables robust

*: authors with equal contributions. Please direct questions to authors@freenome.com.

learning, where X represents the biological data. Note that the confounding covariates may be used to learn f , but are not arguments of f . To this goal, we (1) develop a method named OrthoNormal basis construction In cOnfounding factor Normalization (ONION) for factoring out confounding covariates and (2) apply the Domain-Adversarial Neural Network (DANN) [11] to refrain from learning confounders. The first approach constructs a basis such that some basis vectors span the confounded vector space and the remaining basis vectors span the non-confounded complement vector space. The second method seeks latent spaces that accurately encode the target label and poorly encode confounders. We conduct experiments on both simulated data and real world clinical data to show that ONION and DANN can effectively bridge generalization gaps caused by confounders.

2 Methods

Let X : $n \times p$ be the observed data, where n is the number of observations and p is the number of features. The underlying data generation mechanism involves several factors including the disease status and possibly several confounders. Let Y_1, Y_2, \dots, Y_{k-1} represent the $k - 1$ confounders, where Y_i is $n \times 1$, $i \in \{1, 2, \dots, k - 1\}$, e.g., the age, sex, sample source institution, etc., and let Y_k : $n \times 1$ represent the label of interest, e.g., the clinical disease labels.

2.1 Orthonormal basis construction in confounding factor normalization (ONION)

Assume that X has been centered. The objective of ONION is to rewrite X as $X = X_c + X_n$, in which X_c is associated with Y_i 's for $i = 1, 2, \dots, k - 1$, representing the confounder signal, and X_n is the residual after factoring out covariates, i.e., the normalized data. This is equivalent to finding an orthonormal basis W for \mathbf{R}^p such that when projecting X onto these vector spaces, the association with the confounders can be deconvolved.

$$W = \begin{bmatrix} | & | & \dots & | \\ w_1 & w_2 & \dots & w_p \\ | & | & \dots & | \end{bmatrix}, \quad WW^T = I, \quad \text{where } w_i \in \mathbf{R}^p \text{ denotes the } i^{\text{th}} \text{ basis vector.}$$

$$X = XWW^T = X_c + X_n, \quad \text{where } X_c = \sum_{i < k} Xw_iw_i^T \text{ and } X_n = \sum_{i \geq k} Xw_iw_i^T.$$

There are many methods in the literature to construct W and factorize X . For example, principle component analysis (PCA) sequentially identifies these basis vectors to maximize the variance [12], i.e., $w_1 = \operatorname{argmax}_{\|w\|=1} w^T X^T X w$. However, PCA is unsupervised, and top variations may not be associated with the response. Partial least squares (PLS) and canonical correlation analysis (CCA) are supervised dimension reduction methods and the latent variables can be used as predictors, often giving better performance than standard regression in large p small n scenarios [12, 13, 14]. One can adopt the objective functions in PLS and CCA, but change the orthogonality conditions to form an orthonormal basis to factor out the confounders. The orthonormal constraints allow us to represent data in terms of the basis vectors simply by taking the product as projection. Here we show the modified optimization motivated by PLS:

$$w_i = \operatorname{argmax}_w w^T X^T Y_i Y_i^T X w, \quad \text{s.t. } \|w\| = 1 \text{ and } w^T w_j = 0 \text{ for } j < i < k. \quad (1)$$

Notice that the term $w^T X^T Y_i Y_i^T X w$ finds weight vector that maximizes the covariance between the latent variables Xw and confounder Y_i . The remaining weight vectors w_k, w_{k+1}, \dots, w_p are the basis vectors for the null space of $\{w_1, w_2, \dots, w_{k-1}\}$. Since we are interested in building models to predict Y_k but not the confounders Y_1, Y_2, \dots, Y_{k-1} , we train models on X_n instead of on X . A sequential algorithm using power iteration [15] and applying deflation to satisfy the orthogonality condition in the optimization problem (1) is presented in Algorithm 1. ONION peels away layers of confounders' effects sequentially, hence the acronym.

2.2 Domain-adversarial neural network

Ganin et al.'s Domain-Adversarial Neural Network (DANN) is a feed-forward neural network that shares at least one hidden layer between a target prediction network and a confounder prediction network [11]. Gradients are reversed between the confounder prediction network and the shared layers to remove confounding signal from model representations. See Figure 1 from [11] for a

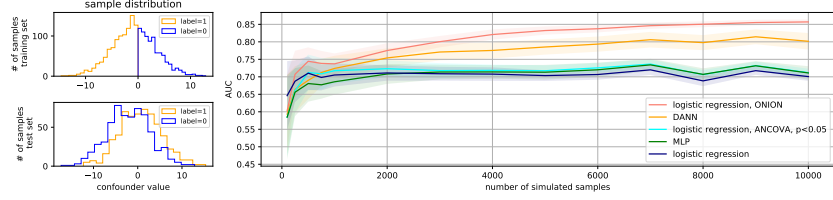


Figure 1: Comparison of no confounder correction versus with correction on balanced test sets using simulated data. The graphs on the left show the distribution of samples with respect to the confounder and labels in the training and test sets when $n = 6000$. The graph on the right compares uncorrected methods to corrective methods as dataset size increases. The curves represent the mean AUC over 50 trials, and the shaded area represents \pm standard error. The method logreg ANCOVA filters features with insignificant association to the label of interest (p -value ≥ 0.05) after removing univariate confounder effects.

network diagram. In our use case, we train $k - 1$ networks $f_{Y_i}(g(X))$, $i = 1, \dots, k - 1$ to predict the $k - 1$ confounders and $f_{Y_k}(g(X))$ to predict the clinical label. g , the shared feature extractor, can be any differential function of X . Training proceeds by alternating stochastic gradient descent updates to:

1. θ_{g_s} and θ_{k_s} , i.e., g 's and f_{Y_k} 's parameters at step s , according to the rules $\theta_{g_{s+1}} = \theta_{g_s} - \alpha \frac{dL_k}{d\theta_{g_s}}$ and $\theta_{k_{s+1}} = \theta_{k_s} - \alpha \frac{dL_k}{d\theta_{k_s}}$, where L_k is the cross entropy loss between predicted and actual clinical labels Y_k .
2. θ_{g_s} and θ_{i_s} , for $i = 1, \dots, k - 1$, i.e., g 's and f_{Y_i} 's parameters at step s , according to the rules $\theta_{g_{s+1}} = \theta_{g_s} + \alpha \sum_{i=1}^{k-1} \frac{dL_i}{d\theta_{g_s}}$ and $\theta_{i_{s+1}} = \theta_{i_s} - \alpha \frac{dL_i}{d\theta_{i_s}}$, where L_i is the loss between predicted and actual confounder Y_i .

3 Experiments

We present results on three datasets to showcase improvements in generalization by correcting for confounders using ONION and DANN. In each scenario, we compare (a) logistic regression (logreg) with and without ONION and (b) an MLP and DANN with the same clinical label prediction architecture using the same train and test data per fold across models.

3.1 Confounded data simulation

We first study confounding in a well-understood setting by simulating confounded data (see supplementary materials). The left panel in Figure 1 shows the distribution of the confounded samples in the first fold of the 5-fold cross validation when $n = 6000$. Notice that the two classes can be perfectly separated by the confounder value in the training set, but not in the test set. Hence, a classifier that learns to predict the confounder will not be robust to confounder value changes in the test set. We compare ONION and DANN against ANalysis of COVariance (ANCOVA),

a univariate feature selection method to filter confounded variables [16]. Figure 1 shows the classification performance in terms of the Area Under the receiver operating characteristic Curve (AUC) as the number of simulated samples varies. The performance gaps between logreg with and without ONION and multilayer perceptron (MLP) versus DANN become apparent as the sample size increases. ANCOVA improves the logreg performance marginally, and becomes impractical as the number of features p increases, so we focus on ONION and DANN in subsequent experiments.

Algorithm 1: ONION

```

initialization  $W = []$ ; (an empty matrix);
 $X_d = X$ ;
for  $i \leftarrow 1$  to  $k - 1$  do
  if  $i > 1$  then
     $X_d = X_d - X^T w_{i-1} w_{i-1}^T$ ;
    Randomly initialize  $u_0$ ;
     $\tau = 0$ ;
    while stopping criterion is not satisfied do
       $\tau = \tau + 1$ ;
       $u_\tau = X_d^T Y_i Y_i^T X_d u_{\tau-1}$ ;
       $u_\tau = u_\tau / \|u_\tau\|$ ;
    end
     $W = [W; u_\tau]$ ; (append  $u_\tau$  to  $W$ )
  end
 $X_n = X - X W W^T$ 

```

3.2 Sequencing data from clinical cancer samples

In both of the following scenarios, we are tasked with predicting whether a patient has cancer or not after sequencing cell-free DNA from the patient’s blood [17, 18]. We featurize the sequencer reads by counting the number of DNA fragments that align to a set of non-overlapping 50 kilobase bins of the human genome, which provides us with 61,775 features. Since we tend to control for known confounders in our clinical datasets, we artificially introduce confounding to study its impact on generalization using methods described in the supplementary materials. The dataset consists of 520 cancer patients and 214 healthy patients. Experiments are conducted with 5-fold cross validation.

3.2.1 Confounding by biological sex

An example of sample collection bias is when most cancer samples are sourced from a particular population subgroup and most healthy samples are sourced from outside that subgroup. We construct a training set where cancer patients are largely female and healthy patients are largely male, whereas the test set is more balanced (see the sample distribution in the supplementary materials). As shown in Table 1, without correcting for confounders (logreg and MLP), the performance is artificially high when the test set is confounded in the same manner as the training set, as is the case when performing k-fold cross validation. However, on the entire test set, without subsampling to mimic training set confounding, uncorrected models perform far worse than corrected models (logreg with ONION and DANN). The reference in Table 1 represents the result using logreg with sex chromosomes removed, which serves as the benchmark if prior knowledge of the features is given.

3.2.2 Confounding by GC bias

Sequencing data often exhibits GC bias, a sample-level technical bias in over- and under-representation of DNA fragments with varying amounts of G and C bases. We construct a scenario in which labels in our training set are confounded by the level of GC bias (see supplementary materials for more detail). In Table 1, we see that GC confounding is more subtle than sex confounding, though the same trends of overinflated metrics without confounder correction and improved performance on unconfounded test sets with confounder correction hold.

4 Discussion and conclusion

In this paper, we propose a novel method, ONION, and apply DANN to correct for confounding factors. Simulated experiments show that both methods outperform univariate ANCOVA screening. Our experiments using clinical cancer data also show that ONION and DANN generalize well, reducing the gap between the performance on the entire test set and a confounded subsampled test set. Experimenting with confounding by biological sex is particularly informative because an unconfounded model should not build predictions upon inferring sex using the sex chromosomes, chrX and chrY. We indeed notice that the logistic regression model without ONION has opposite signs on chrX and chrY weights (see supplementary materials), whereas using ONION removes this trend. A direction of future work is to incorporate generative networks and data augmentation into our models [19, 20, 21] and determine DANN’s ability to remove nonlinear confounding effects of varying degrees. Without confounder correction methods, the gap between the performance on the entire test set and the confounded test in our simulated and clinical datasets set points out the ease of mistakenly presenting inaccurate performance in the machine learning community. We hope this work not only equips researchers with new methods to control for confounding, but also spurs additional work to detect and correct for confounding in biological datasets.

Acknowledgments

The authors gratefully acknowledge Lena Cheng, Riley Ennis, Signe Fransen, Girish Putcha and David Weinberg (in alphabetical order) for their extensive suggestions, feedback, and editorial support.

Table 1: Confounding experiments using clinical cancer data. In the sex confounding experiment, reference represents logreg trained without sex chromosomes. In the GC confounding experiment, reference represents logreg trained after LOWESS GC correction. These references serve as benchmark solutions when prior domain knowledge is given. The confounded test set is the maximally sized subset of the entire test set with the same level of confounding as the training set, which represents using k-fold cross validation on confounded data. ONION and DANN are able to correct for confounding and often achieve similar performance to the reference.

method	Sex: mean AUC (SD)		GC: mean AUC (SD)	
	entire test set	confounded test set	entire test set	confounded test set
logreg	0.59 (0.04)	1.00 (0.00)	0.82 (0.08)	0.98 (0.01)
logreg, ONION	0.91 (0.01)	0.68 (0.06)	0.93 (0.02)	0.88 (0.07)
MLP	0.61 (0.06)	0.79 (0.25)	0.82 (0.11)	0.93 (0.09)
DANN	0.78 (0.07)	0.80 (0.08)	0.86 (0.05)	0.93 (0.07)
reference	0.92 (0.02)	0.95 (0.01)	0.92 (0.02)	0.86 (0.04)

References

- [1] Maxwell W Libbrecht and William Stafford Noble. Machine learning applications in genetics and genomics. *Nature Reviews Genetics*, 16(6):321, 2015.
- [2] Jeffrey T Leek, Robert B Scharpf, Héctor Corrada Bravo, David Simcha, Benjamin Langmead, W Evan Johnson, Donald Geman, Keith Baggerly, and Rafael A Irizarry. Tackling the widespread and critical impact of batch effects in high-throughput data. *Nature Reviews Genetics*, 11(10):733, 2010.
- [3] Nathan Wan, David Weinberg, Tzu-yu Liu, Katherine Niehaus, Daniel Delubac, Ajay Kannan, Brandon White, Eric Ariazi, Mitch Bailey, Marvin Bertin, Nathan Boley, Derek Bowen, James Cregg, Adam Drake, Riley Ennis, Signe Fransen, Erik Gafni, Loren Hansen, Yaping Liu, Gabriel L Otte, Jennifer Pecson, Brandon Rice, Gabriel E Sanderson, Aarushi Sharma, John St. John, Catherina Tang, Abraham Tzou, Leilani Young, Girish Putcha, and Imran S Haque. Machine learning enables detection of early-stage colorectal cancer by whole-genome sequencing of plasma cell-free dna. *bioRxiv*, 2018. doi: 10.1101/478065. URL <https://www.biorxiv.org/content/early/2018/11/24/478065>.
- [4] Vathany Kulasingam and Eleftherios P Diamandis. Strategies for discovering novel cancer biomarkers through utilization of emerging technologies. *Nature Reviews Clinical Oncology*, 5(10):588, 2008.
- [5] Magdalena Chechlinska, Magdalena Kowalewska, and Radoslaw Nowak. Systemic inflammation as a confounding factor in cancer biomarker discovery and validation. *Nature Reviews Cancer*, 10(1):2, 2010.
- [6] Kangway V. Chuang and Michael J. Keiser. Adversarial controls for scientific machine learning. *ACS Chemical Biology*, 13(10):2819–2821, 2018. doi: 10.1021/acscchembio.8b00881. URL <https://doi.org/10.1021/acscchembio.8b00881>.
- [7] Sara Mostafavi, Alexis Battle, Xiaowei Zhu, Alexander E. Urban, Douglas Levinson, Stephen B. Montgomery, and Daphne Koller. Normalizing rna-sequencing data by modeling hidden covariates with prior knowledge. *PLoS ONE*, 8(7):e68141.
- [8] W. Evan Johnson, Cheng Li, and Ariel Rabinovic. Adjusting batch effects in microarray expression data using empirical bayes methods. *Biostatistics*, 8(1):118–127, 2007.
- [9] William S. Cleveland. Robust locally weighted regression and smoothing scatterplots. *Journal of the American Statistical Association*, 74(368):829–836, 1979.
- [10] Yuval Benjamini and Terence P. Speed. Summarizing and correcting the gc content bias in high-throughput sequencing. *Nucleic Acids Research*, 40(10):e72, 2012.
- [11] Yaroslav Ganin, Evgeniya Ustinova, Hana Ajakan, Pascal Germain, Hugo Larochelle, François Laviolette, Mario Marchand, and Victor Lempitsky. Domain-adversarial training of neural networks. *The Journal of Machine Learning Research*, 17(1):2096–2030, 2016.
- [12] Jerome Friedman, Trevor Hastie, and Robert Tibshirani. *The elements of statistical learning*, volume 1. Springer series in statistics New York, NY, USA, 2001.
- [13] Sijmen de Jong. SIMPLS: an alternative approach to partial least squares regression. *Chemometrics and intelligent laboratory systems*, 18(3):251–263, 1993.
- [14] Harold Hotelling. Relations between two sets of variates. *Biometrika*, 28(3/4):321–377, 1936.

- [15] Todd K Moon and Wynn C Stirling. *Mathematical methods and algorithms for signal processing*, volume 1. Prentice hall Upper Saddle River, NJ, 2000.
- [16] Bradley Huitema. *The analysis of covariance and alternatives: Statistical methods for experiments, quasi-experiments, and single-case studies*, volume 608. John Wiley & Sons, 2011.
- [17] Matthew W Snyder, Martin Kircher, Andrew J Hill, Riza M Daza, and Jay Shendure. Cell-free dna comprises an in vivo nucleosome footprint that informs its tissues-of-origin. *Cell*, 164(1):57–68, 2016.
- [18] Viktor A Adalsteinsson, Gavin Ha, Samuel S Freeman, Atish D Choudhury, Daniel G Stover, Heather A Parsons, Gregory Gydush, Sarah C Reed, Denisse Rotem, Justin Rhoades, et al. Scalable whole-exome sequencing of cell-free dna reveals high concordance with metastatic tumors. *Nature communications*, 8(1):1324, 2017.
- [19] Ian Goodfellow, Jean Pouget-Abadie, Mehdi Mirza, Bing Xu, David Warde-Farley, Sherjil Ozair, Aaron Courville, and Yoshua Bengio. Generative adversarial nets. In *Advances in neural information processing systems*, pages 2672–2680, 2014.
- [20] Stefan Bonn, Pierre Machart, Mohamed Marouf, Daniel Sumner Magruder, Vikas Bansal, Christoph Kilian, and Christian F Krebs. Realistic in silico generation and augmentation of single cell rna-seq data using generative adversarial neural networks. *bioRxiv*, page 390153, 2018.
- [21] Hongyi Zhang, Moustapha Cisse, Yann N Dauphin, and David Lopez-Paz. mixup: Beyond empirical risk minimization. *arXiv preprint arXiv:1710.09412*, 2017.
- [22] Michael W Browne. The maximum-likelihood solution in inter-battery factor analysis. *British Journal of Mathematical and Statistical Psychology*, 32(1):75–86, 1979.
- [23] Arto Klami, Seppo Virtanen, and Samuel Kaski. Bayesian canonical correlation analysis. *Journal of Machine Learning Research*, 14(Apr):965–1003, 2013.
- [24] Broad Institute. Picard tools. <http://broadinstitute.github.io/picard/>, (Accessed: 2018; version 2.13.2).

5 Supplementary Materials

5.1 Clinical cancer dataset

The clinical samples were sourced from various academic institutions and sample collection companies from retrospective studies. These samples include colorectal cancer samples, the majority of which are early stage cancer samples, and healthy samples as controls.

	Healthy	Cancer	Total
Female	156	245	401 (55%)
Male	58	275	333 (45%)
Total	214 (29%)	520 (71%)	734

We preprocess the 50 kilobase bin fragment counts by multiplying each sample i 's counts, denoted c_i , by $\frac{k}{\text{sum}(c_i)}$ (k is a constant) to simulate an equal number of reads per sample. We then clip and standardize the counts based on the training set, and apply the learned mean, standard deviation, and outlier thresholds to the test set. We clip outlier counts to the 99th percentile count per feature.

5.2 Model hyperparameters

Due to the small number of samples, we restrict the size of the MLP and DANN architectures. In clinical cancer experiments, we use the first 200 principle components of PCA to reduce input dimensionality and use one hidden layer of 20 units. In DANN, we use a hidden layer of 20 units to predict the confounder of interest that uses the 20 unit hidden layer from the clinical label prediction network as input. In all comparisons, we fix hyperparameters for fair comparison. We train models using cross entropy loss for categorical variables and mean squared error for continuous variables. We choose the best performing model based on a validation set, using accuracy as the model metric for MLPs and using $L_k - \sum_{i=1}^{k-1} \alpha_i L_i$ (a weighted sum of the clinical label prediction loss and the negative confounder prediction losses) for DANNs. Models are trained for 6,000 iterations with a batch size of 64 for the clinical label prediction network using Adam and a learning rate of 0.005. DANN's confounder prediction network is trained three steps for every clinical label prediction update. Everything is kept the same for the simulated data task, except the hidden layer in both the MLP and DANN is 5 units rather than 20.

5.3 Confounding procedure

5.3.1 Simulated confounding

We extend the inter-battery factor analysis model studied in [22, 23] to formulate a simulation model for generating confounded data.

$$\begin{aligned}
 Z_i &\sim N(0, I_d), \quad i = 1, 2, \dots, k \\
 W_{x_i} &: d \times p, \quad W_{x_i}(i, j) \sim N(0, 1), \quad i = 1, 2, \dots, k \\
 W_{y_i} &: d \times 1, \quad W_{y_i}(i) \sim N(0, 1), \quad i = 1, 2, \dots, k \\
 \mathcal{E}_X &\sim N(0, \sigma^2 I_p) \\
 \mathcal{E}_{y_i} &\sim N(0, \sigma^2), \quad i = 1, 2, \dots, k \\
 \alpha &= [\alpha_1, \alpha_2, \dots, \alpha_k] \sim \text{Dir}([s_1, s_2, \dots, s_k]) \\
 X &= \sum_{i=1}^k Z_i W_{x_i} + \mathcal{E}_X \\
 Y_i &= Z_i W_{y_i} + \mathcal{E}_{Y_i}, \quad i = 1, 2, \dots, k-1 \\
 Y_k &= \mathbf{1} \left\{ \sum_{i=1}^{k-1} \alpha_i Y_i + \alpha_k Z_k W_{y_k} + \mathcal{E}_{y_k} > 0 \right\},
 \end{aligned} \tag{2}$$

in which $\mathbf{1}$ is the indicator function, $N(\mu, \Sigma)$ represents the normal distribution with mean μ and covariance Σ , and $\text{Dir}([s_1, s_2, \dots, s_k])$ represents the Dirichlet distribution with concentration



Figure 2: Sample distribution in the experiments of sex confounding.

parameters $[s_1, s_2, \dots, s_k]$. Z_i 's are the shared latent variables between the independent and dependent variables, and W_{x_i} and W_{y_i} are used for constructing linear combinations of the latent variables to synthesize X_i and Y_i , with additive noise \mathcal{E}_X and \mathcal{E}_{y_i} . The vector α sampled from the Dirichlet distribution controls for the confounding level, i.e., the larger the α_j , the higher impact the confounder Y_j on the true label of interest, Y_k .

We set $d = 20$, $p = 300$, $\sigma = 2$, $k = 2$ and $s_1 = 40$, $s_2 = 50$ in our experiments. To synthesize n samples for the experiment, we first sample W_{x_i} , W_{y_i} and α once, and repeatedly sample Z_i 's for n times to construct X and Y_i 's. We then filter the samples to create skewed distribution in the training set by only allowing samples that have $Y_1 < 0$ and $Y_2 = 1$ or $Y_1 \geq 0$ and $Y_2 = 0$, while the test set is kept balanced.

5.3.2 Confounding by sex

We construct a training set where cancer patients are largely female and healthy patients are largely male, whereas the test set is balanced. The training set is obtained by randomly removing the male cancer patients and female healthy patients with probability 0.9. Figure 2 shows the sample distributions in one of the 5 folds.

5.3.3 Confounding by GC bias

Genomes consist of a heterogeneous mix of chemicals called nucleotides with varying electrochemical properties. These chemicals are guanosine (G), cytosine (C), adenosine (A), and thymidine (T). Guanosine and cytosine have the potential to form three hydrogen bonds while adenosine and thymidine make two. This difference in bonding results in different behavior of DNA fragments based on their nucleotide composition. In particular, the processes that convert DNA molecules into modern DNA sequencer output introduce biases related to the GC-content of the input molecules, which is known as GC bias.

We construct a scenario where labels in our training set are confounded by the level of GC bias. To measure GC bias, we use the Picard Tools metric of AT dropout $dropout_{AT} = \sum_{gc=0}^{50} \max(E_{gc} - O_{gc}, 0)$, where gc represents percent GC, $E_{gc} = \frac{len(R_{gc})}{len(genome)}$ (the expected number of reads overlapping the region R_{gc} , the union of 100 base pair windows of the genome with GC percentage gc , assuming uniform coverage of the genome), and $O_{gc} = \frac{\sum_r I_{r \cap R_{gc}}}{count(reads)}$, where the numerator represents the number of reads overlapping regions R_{gc} [24]. We focus on AT dropout because our particular sequencing procedure results in under-representation of AT-rich fragments. The sample distributions in one fold among the 5 folds are shown in Figure 3. The confounded training set is obtained by randomly filtering healthy samples with low $dropout_{AT}$ (below 3.5) and cancer samples with high $dropout_{AT}$ (above 3.5) with probability 0.9. The sex chromosomes are removed when comparing all methods in the GC confounding experiments, since LOWESS GC correction does not perform well when chrX and chrY exist in the feature set.

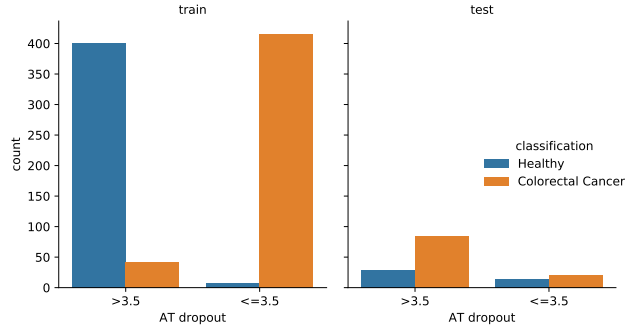


Figure 3: Sample distribution in the experiments of GC bias confounding.

5.4 Additional analysis results

We examine the weights in the logistic regression model with and without ONION in the sex confounding experiment, Table 1. Figure 4 shows the weights corresponding to each feature, sorted by chromosome number. The weights associated with chrX and chrY have opposite signs in the model trained without ONION. This suggests that the model relies on sex (the confounder) to make predictions. This pattern does not occur when using the ONION, which implies the model does not use confounders for prediction.

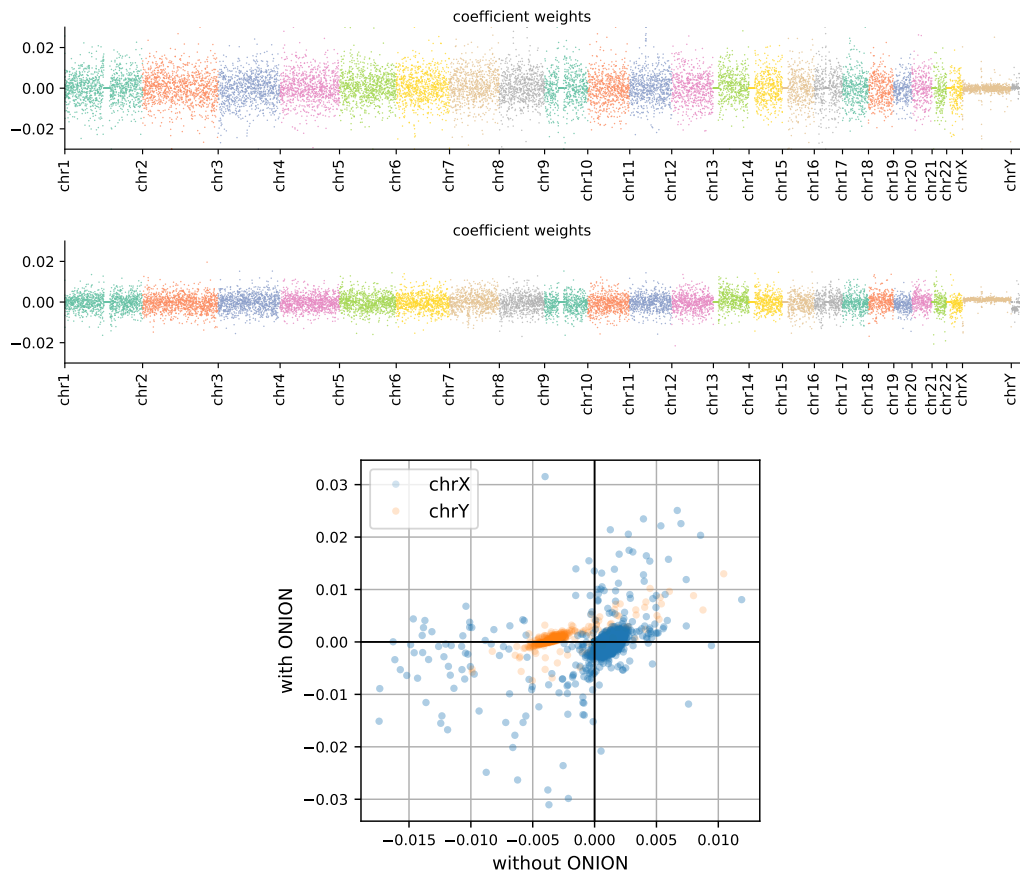


Figure 4: Classifier weights associated with each feature in the sex confounding experiment using logistic regression model with (the top panel) and without ONION (the middle panel). Note that signs of the weights associated with chrX and chrY in logreg without ONION are opposite, whereas they are all centered around zero in the model with ONION. This is further illustrated in the bottom panel, where we plotted the weights on chrX and chrY in the logreg model with and without ONION.